

WaymoQA: A Multi-View Visual Question Answering Dataset for Safety-Critical Reasoning in Autonomous Driving

Seungjun Yu
seungjunyu@kaist.ac.kr
KAIST
Seoul, Republic of Korea

Seonho Lee
glanceyes@kaist.ac.kr
KAIST
Seoul, Republic of Korea

Namho Kim
knhnh@hanyang.ac.kr
Hanyang University
Seoul, Republic of Korea

Jaeyo Shin
jaeyo_shin@kaist.ac.kr
KAIST
Seoul, Republic of Korea

Junsung Park
jshackist@kaist.ac.kr
KAIST
Seoul, Republic of Korea

Wonjeong Ryu
petac@kaist.ac.kr
KAIST
Seoul, Republic of Korea

Raehyuk Jung
mulnyangi@naver.com
KAIST
Seoul, Republic of Korea

Hyunjung Shim*
kateshim@kaist.ac.kr
KAIST
Seoul, Republic of Korea

Abstract

Recent advancements in multimodal large language models (MLLMs) have shown strong understanding of driving scenes, drawing interest in their application to autonomous driving. However, high-level reasoning in safety-critical scenarios, where avoiding one traffic risk can create another, remains a major challenge. Such reasoning is often infeasible with only a single front view and requires a comprehensive view of the environment, which we achieve through multi-view inputs. We define Safety-Critical Reasoning as a new task that leverages multi-view inputs to address this challenge. Then, we distill Safety-Critical Reasoning into two stages: first resolve the immediate risk, then mitigate the decision-induced downstream risks. To support this, we introduce WaymoQA, a dataset of 35,000 human-annotated question-answer pairs covering complex, high-risk driving scenarios. The dataset includes multiple-choice and open-ended formats across both image and video modalities. Experiments reveal that existing MLLMs underperform in safety-critical scenarios compared to normal scenes, but fine-tuning with WaymoQA significantly improves their reasoning ability, highlighting the effectiveness of our dataset in developing safer and more reasoning-capable driving agents. Our code and data are provided in <https://github.com/sju001/WaymoQA>

Keywords

WaymoQA, Safety-Critical Autonomous Driving, Driving Visual Question Answering

1 Introduction

Recent progress in Multimodal Large Language Models (MLLMs) have demonstrated impressive performance across a wide spectrum of vision-language tasks, including image captioning, visual reasoning, and visual question answering (VQA) [1, 43, 67, 76]. These capabilities have naturally extended into autonomous driving, where MLLMs are being explored for end-to-end driving pipelines, scenario generation, and vision-language action modeling [17, 19,

22, 26, 43, 51]. Among these efforts, Driving Question Answering (Driving QA) has emerged as a promising paradigm for equipping autonomous agents with high-level scene understanding and decision-making capabilities.

In VQA, the design of the dataset is the primary factor that determines the measurable capacity of models. [4, 29, 46]. Early efforts in Driving QA datasets, such as DRAMA [44] and DriveLM [55], adopted a single-view setting. However, the increasing complexity of real-world driving and the advent of multi-sensor perception systems have highlighted the importance of multi-view scene understanding. This led to the development of datasets like NuScenes-QA [49] and NuPlan-QA [48], which integrate multi-camera inputs to better capture spatial relationships and inter-agent dynamics, reflecting the perceptual richness of modern autonomous systems.

Despite this progress, existing datasets [18, 36, 40] still focus primarily on normal scenarios and overlook safety-critical events [68]. These events are rare but highly consequential. Examples include pedestrians suddenly emerging from occlusions, abrupt braking triggered by unforeseen obstacles, or conflicts between multiple agents at intersections. The true reliability of an autonomous driving system is not determined by its performance in normal scenarios but by its behavior in these unpredictable, dangerous moments, specifically safety-critical scenarios. Recent works such as NAVSAFE [54] have recently recognized this and emphasized the importance of evaluating models on safety-critical scenarios. Accordingly, recent benchmarks such as DVBench [68] and VRU-Accident [32] developed safety-critical driving QA benchmarks.

However, these works [32, 68] have three key limitations. **(L1)** They are designed exclusively for evaluation and do not include training data, preventing MLLMs from learning safety-critical reasoning directly from examples. A dedicated training dataset is essential for MLLMs to learn safety-critical reasoning. **(L2)** Like the early Driving QA works, they rely on single-view inputs, which limits the understanding of complex safety-critical scenarios. A single-view system can miss blind spots or occluded agents. **(L3)** Consequently, and **most critically**, they lack support for high-level reasoning across the full autonomy stack, from perception

*Corresponding Author.

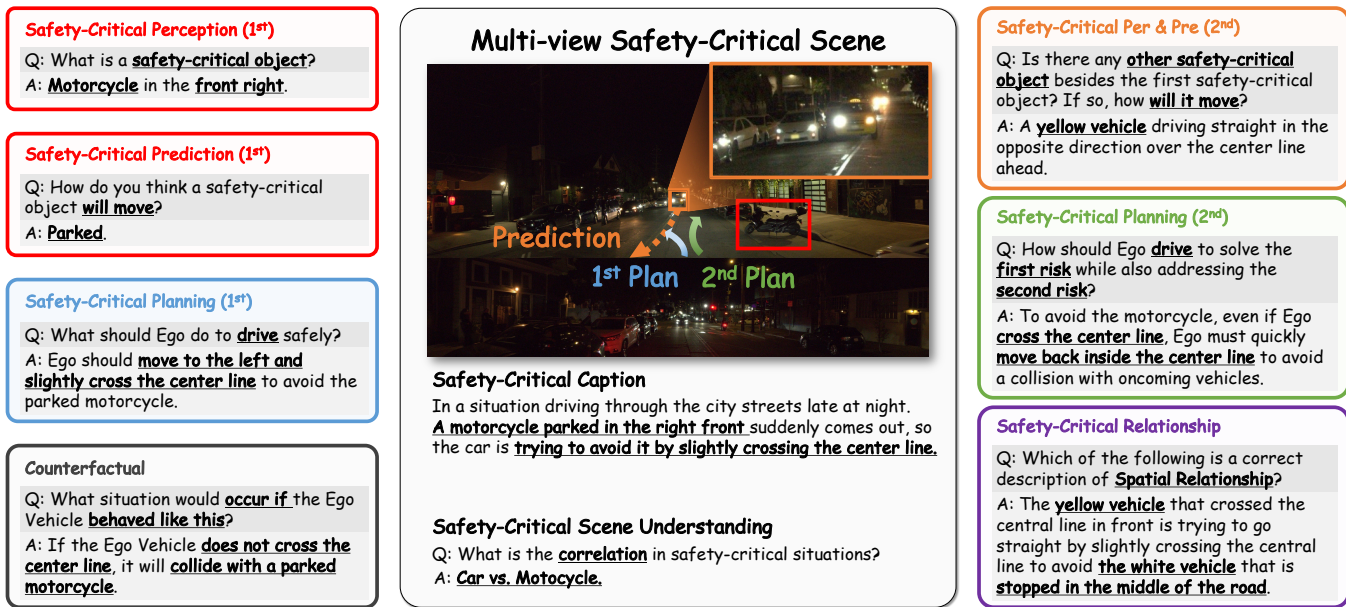


Figure 1: WaymoQA overview: multi-view scenes and two-stage reasoning (Perception → Prediction → Planning) under compounding risks. The agent first detours around a parked motorcycle, then returns to avoid an oncoming car. *Safety-Critical Relationship* questions probe alternative actions; safety-critical relationship questions capture spatial relations among agents.

to behavior prediction and risk-aware motion planning. As shown in Fig. 2, the same scene yields opposite decisions under different view coverage. With a single front view the model concludes that a lane change is both feasible and safer. With multi view the rear right vehicle becomes visible, the lane change becomes infeasible, and slowing down becomes safer. This failure arises because limited view coverage produces an incomplete feasibility set and an incorrect risk ranking, which manifests as missing action and consequence reasoning. Such high-level reasoning, which is essential in safety-critical scenes, is largely missing from existing approaches.

To address these limitations, we introduce WaymoQA, the first training-enabled, safety-critical multi-view driving QA dataset. Built from long-tail scenarios in the Waymo End-to-End dataset [64] and filtered using U.S. NHTSA (National Highway Traffic Safety Administration) [64] safety criteria, WaymoQA consists of 35,000 human-written question-answer pairs, covering safety-critical videos and key frames that are manually selected.

To address (L1) the absence of a training set, we release WaymoQA with 28,585 training set and 6,415 test set. The dataset supports two formats, multiple-choice questions for test and open-ended questions for train. Both are included in the training set to enable in-distribution validation.

To tackle (L2) the information loss from single front frame view, WaymoQA resolves scenes using multi view inputs at each time step. We aggregate eight synchronized views (front left, front center, front right, side left, side right, rear left, rear center, rear right) so that occlusions are reduced and the spatial field of view is expanded. This multi-view configuration expands the field of view, admits more evidence, and yields more accurate scene understanding, thereby providing the **evidential basis** required for reliable

high-level reasoning. In short, the multi-view design provides the essential foundation for a principled formulation of safety-critical reasoning in autonomous driving.

To address (L3) the lack of high-level reasoning, building on this foundation, we adopt two complementary strategies. **First**, we explicitly define a new task, *Safety-Critical Reasoning*, structured into two progressive stages, and design 70% of WaymoQA to require such high-level reasoning. Stage 1 focuses on resolving the immediate risk as the model detects the safety-critical object, predicts its trajectory, and selects the safest feasible action. Stage 2 reasons for secondary risks that may be triggered by Stage 1 action, reflecting real-world driving where mitigating one hazard can introduce another. As shown in Fig. 1, the ego first passes a parked motorcycle on the front right by briefly crossing the center line and then promptly returns inside the line to avoid an oncoming vehicle. These compounded decisions exemplify the two-stage *Safety-Critical Reasoning* elicited by WaymoQA. **Second**, we leverage the complementary strengths of video and image to enrich reasoning signals as shown in Fig. 5. Video QA captures how events unfold and verifies what actually occurred, assessing both the motion of the safety-critical object and the ego response. Image QA presents a single key frame from the same situation and invites decision-oriented and counterfactual queries that are not tied to the realized timeline. While departing from the single realized path in the video, Image QA broadens the space of alternative actions and near term outcomes for the same scene. Together, the two-stage formulation and the complementary video and image views address (L3) by making action and consequence reasoning explicit, broadening the decision space, and improving high-level understanding of safety-critical scenes.

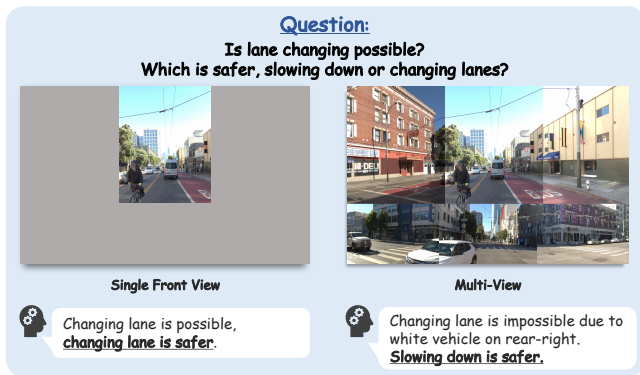


Figure 2: Comparison across Difference Views of Same Scene.

Comprehensive experiments on state-of-the-art MLLMs reveal that their understanding of safety-critical scenes is, on average, about 20% lower than their understanding of normal scenes. However, after fine-tuning on the WaymoQA training set, we observed not only significant gains across overall tasks, approximately +16.8% accuracy on Image QA and +16.3% on Video QA, but also reduced gap between normal and safety-critical scenes. These results demonstrate that WaymoQA is an effective solution for improving an MLLMs’ ability to make correct decisions in safety-critical situations, and point to a clear path for general-purpose MLLMs to further close the remaining gap between safety-critical reasoning and normal reasoning. Our contributions are summarized as follows:

- **Task definition.** We define a new task of safety-critical reasoning under multi-view inputs within vision and language understanding for autonomous driving.
- **Dataset.** We present WaymoQA, the first safety-critical and multi-view driving QA dataset with a training split, enabling research beyond evaluation only.
- **Analysis and findings.** Through systematic analyses and experiments, we characterize MLLMs’ safety-critical understanding and show that training data markedly improve this capability.

2 Related Works

MLLM in Autonomous Driving. Multimodal large language models (MLLMs) exhibit strong high-level reasoning across tasks [6, 24, 41, 56], motivating their adoption in autonomous driving [8, 13, 75]. Recent work moves beyond perception/captioning toward language-driven planning: DriveVLM [58] couples MLLMs with conventional driving models for spatial reasoning, while DriveGPT4 [65] produces text-level actions from video. HiLM-D [14] enhances perception/prediction via high-resolution details, and DME-Driver [23] adds 3D scene understanding and human decision patterns for improved planning. Generative approaches such as GAIA-1 [25] synthesize full scenarios conditioned on video/actions, whereas GPT-Driver [45] casts motion planning as language modeling to build a specialized planner. Agentic systems further expand capabilities, e.g., SurrealDriver [28], and OpenDriveVLA [74] jointly outputs actions and trajectories by training on heterogeneous datasets.

Finally, EMMA [27] converts MLLM text outputs into trajectories in a model-agnostic manner. Overall, the field is shifting from scene narration to decision-making tightly coupled with perception and control.

Safety-Critical Autonomous Driving. Safety-critical driving is challenging due to rarity, diversity, and the need for causal reasoning. Scenario generation has progressed from planner-driven stress testing—STRIVE [50], CTG [72], and CTG++ [71]—to adversarial/controllable diffusion and causal composition for closed-loop traffic [37, 63], with RL-based synthesis also explored [39]. To better match end-to-end stacks that consume raw visuals, vision-in-the-loop efforts include anomaly analysis in real videos (DoTA [66]) and safety-focused data generation/benchmarks such as CTAD [42], DeepAccident [59], and simulator-scale synthesis via ChatScene in CARLA [15, 69]. More recent works improve realism and multi-view E2E alignment, with ADV2 [35] fine-tuning Open-Sora [70], SafeMVDriver [73] leveraging GRPO [52], and MM-AU [16] adding causal rationales and prevention descriptions.

3 WaymoQA Dataset

In this section, we describe the overall design of the WaymoQA dataset, which serves as the foundation for the safety-critical reasoning task. Figure 3 illustrates the structured data construction process, which ensures high-quality annotations and balanced QA distribution across formats and reasoning categories.

3.1 Classifying Safety-Critical Scenes and Key Frames

The Waymo End-to-End (Waymo E2E) dataset [64] encompasses a variety of long-tail driving scenarios, only a subset of which involves safety-related events. Because identifying safety-critical situations can be subjective, we apply an objective filtering process based on the 47 pre-crash scenarios defined by the U.S. NHTSA (National Highway Traffic Safety Administration) [3]. This ensures consistent and reproducible selection of safety-critical scenes. After filtering scenario, we extract key frames from the video sequences to build the Image QA component. Safety-critical events typically occur within a short temporal window. For example, in a 22-second scenario from the Waymo End-to-End data, the safety-critical moment lasts on average only about 2–4 seconds. If QA dataset are generated solely from these brief safety-critical moments, the dataset would overrepresent critical moments and hinder the model’s ability to generalize to normal driving conditions. To avoid this imbalance, we curate key frames that maintain an even distribution between normal and safety-critical contexts. We follow three strict guidelines for key frame selection:

- (1) Maintain a 2:3 **ratio** of normal frames to safety-critical frames.
- (2) The selected frames should not be too similar to each other, and the time interval between any two selected frames should be **at least 1 second timestep**.
- (3) Select **at least 5 frames** from each video.

Using these carefully designed guidelines, we identify safety-critical scenarios and select their key frames from the Waymo End-to-End dataset.

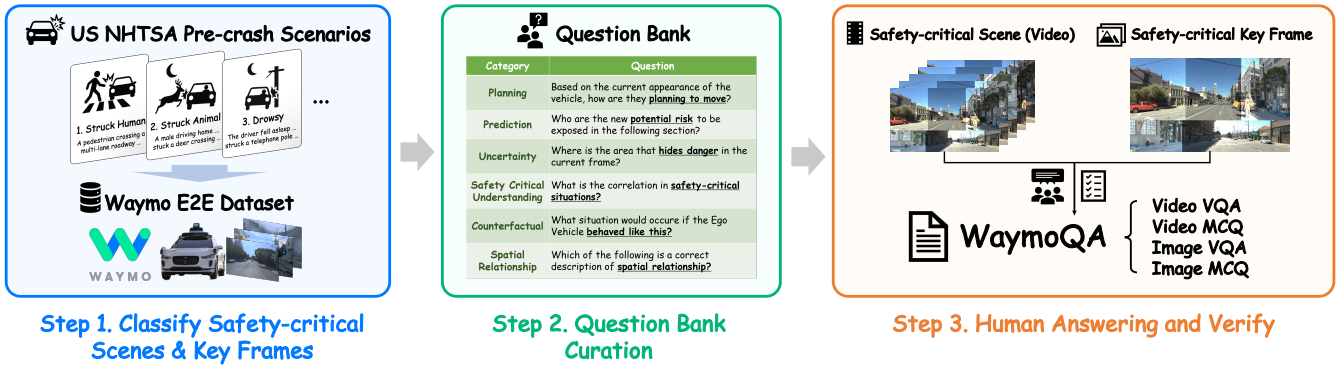


Figure 3: Overview. A three-step process: (1) filter Waymo End-to-End sequences using U.S. NHTSA pre-crash scenario types [3] and select balanced safety-critical key frames; (2) construct a structured QA bank covering core reasoning skills; (3) complete human answering and verification to produce Video/Image VQA and MCQ splits.

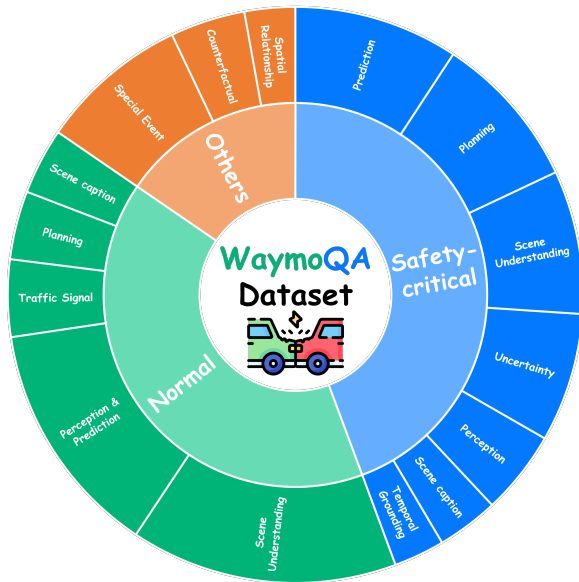


Figure 4: VQA distribution in the WaymoQA dataset.

3.2 Question Bank Curation

Before generating the QA pairs, we construct a **62 item question bank** to systematize reasoning and scene understanding for long-tail, safety-critical scenarios. The question bank follows a three-level hierarchy (Fig. 4):

- **Format:** Video or Image.
- **Scene:** Safety-Critical, Normal, or Others.
- **Task:** One of 12 predefined reasoning categories.

The reasoning categories are *Caption*, *Scene Understanding*, *Perception*, *Prediction*, *Planning*, *Uncertainty*, *Counterfactual*, *Special Event*, *Spatial Relationship*, *Temporal Grounding*, and *Traffic Signal*. Each question in the bank is labeled with structured metadata, for example, a question might be annotated as {"Format": "Video", "Scene": "Safety-Critical Planning"}. Further details and

examples of these question categories are provided in the supplementary material.

3.3 Two-Stage Safety-Critical Reasoning

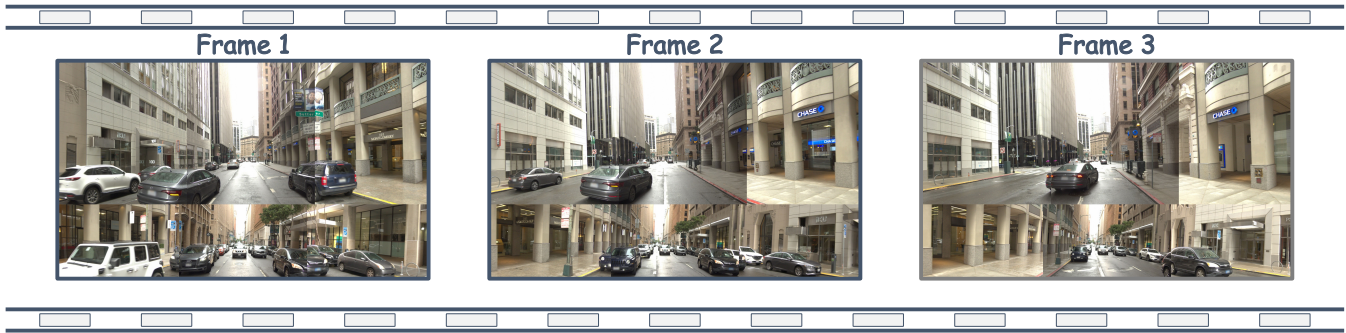
Safety-critical driving requires reasoning over both the immediate risk and the downstream consequences of chosen actions, as explained in Sec. 1 and illustrated in Fig. 1. To capture this reasoning process, we structure the task into two dependent stages that explicitly model action-consequence reasoning. Stage 1 identifies the safety-critical scene, perceives the safety-critical object, predicts its behavior, and decides the safest feasible action to resolve the current risk. Stage 2 is *conditioned on the Stage 1 action*. Given the updated situation after executing the Stage 1 choice, this stage reasons about newly exposed or induced secondary risks and selects the safest action that achieves the Stage 1 objective while mitigating the new threat.

For three reasons, a two stage formulation is essential rather than a single stage. First, this structure forces action and consequence reasoning because the Stage 2 query cannot be answered without committing to a Stage 1 decision. Second, it disambiguates error sources by separating present resolution from downstream foresight, enabling more precise failure analysis. Third, it enables counterfactual branching, where different Stage 1 choices yield different Stage 2 questions and answers.

In short, Stage 2 is not merely single-step reasoning on the next predicted frame. It is a decision-conditioned assessment of secondary risk induced by the Stage 1 action, enabling deeper understanding in long tail safety-critical scenarios and providing clearer diagnostics for perception, prediction, and planning.

3.4 Video vs. Image QA

Safety-critical scenarios are rare in practice despite their importance, which limits the coverage attainable when constructing reasoning data from video alone. We therefore leverage two complementary perspectives. Video QA enables temporal reasoning about what actually occurred, while Image QA extends safety-critical reasoning by exploring alternative decisions from a single key frame as shown in Fig. 5.



| Scene Understanding | | | |
|--|--|--|--|
| <p>Video Summary : Ego vehicle proceeded straight while avoiding a parked vehicle on the left side of a four-lane road in the city. There was a vehicle changing to the right lane from the left front road into the road Ego vehicle was driving on, and since the distance between that vehicle and mine was close, Ego vehicle changed lanes from left to right.</p> <p>Image Caption : A situation where Ego vehicle is changing from the second right turn-only lane to the first right turn lane on a four-lane road in the city. A gray vehicle in the left front is changing lanes to the right to move in front of the vehicle.</p> | | | |
| Video QA | Image QA | | |
| <p>Question : How did the safety-critical object move and how did the ego vehicle behave?</p> <p>Answer : The safety-critical object moved in front of the vehicle by changing lanes from left to right, the Ego-vehicle changed lanes to the right twice.</p> | <p>Question : What actions are currently possible?</p> <p>Answer : Go straight, stop, change to the right lane</p> | <p>Question : What should Ego do to drive safely?</p> <p>Answer : The ego vehicle should slow down to avoid colliding with the vehicle merging from the left.</p> | <p>Question : Is lane changing possible? Which is safer, slowing down or changing lanes?</p> <p>Answer : Lane changing is possible, slowing down is safer.</p> |
| <p>Question : Who is responsible in a safety-critical situation? What is the cause?</p> <p>Answer : A gray vehicle changing lanes in the left front did so abruptly without maintaining a safe distance and changed lanes consecutively.</p> | <p>Question : If the Ego vehicle behaved like this, what situation might occur?</p> <p>Answer : If the Ego vehicle continues straight without slowing down, a collision with a gray vehicle changing lanes ahead will occur.</p> | <p>Question : What situation might have occurred if the Ego vehicle had behaved this way?</p> <p>Answer : If the Ego vehicle had not slowed down, a collision would have occurred with the vehicle changing lanes.</p> | |

Figure 5: Examples of Video/Image QA in WaymoQA. The video QA focuses on the realized temporal sequence, while the image QA, given a single key frame, supports broader, decision-oriented questions about feasible actions and near-term outcomes. Pairing image-based and video-based QA increases the diversity of reasoning signals for rare, long-tail safety-critical scenarios.

In the example of Fig. 5, a vehicle cuts in from the left as the ego changes lanes, and the ego moves to the right lane to avoid a collision. From a single key frame of the same situation, Image QA can ask which actions are feasible at this time, which option is safer given visible risks, and whether a lane change is possible or slowing down is preferable. Since these questions move beyond the single realized path, they expand the set of alternative actions and near term outcomes for the same scene.

Combining the two perspectives increases the diversity of reasoning signals for rare long-tail safety-critical events. This also enables more robust learning and evaluation even when scenario data are limited.

3.5 Formats and Evaluation

WaymoQA provides two formats. Open-ended QA pairs are used for train, while multiple-choice questions (MCQ) are used for test

and validation. We adopt a four-option MCQ design and write all options by humans. The position of the correct answer is uniformly distributed across the four slots to avoid position bias and reduce random guessing. This choice avoids LLM-as-a-judge scoring and enables objective accuracy evaluation with a fixed answer key. Prior work [7, 9, 61] has shown that LLM-based grading can exhibit biases, such as a preference for longer answers regardless of correctness and a tendency to favor responses written in a style similar to the evaluator. Our MCQ setup is therefore intended to provide a consistent and fair evaluation without relying on an LLM grader.

3.6 Human Answering and Verification

Recent studies have begun to automatically generate driving QA data with MLLMs [30, 47]. Such data do not create new information but rather distill what a pretrained model already contains, forming

Table 1: Comparison of driving QA datasets and reasoning coverage. The following abbreviations are used: reasoning dimensions—Perception(Per.), Normal Reasoning(Nor.Rea.), Safety-Critical Reasoning(SC.Rea.), Two-Stage Safety-Critical Reasoning(2SS.Rea.). WaymoQA uniquely covers all listed dimensions while providing both Image/Video QA with a 35K-item scale.

| Dataset | Normal | Safety-Critical | Multi View | Train Data | Video | Image | Per. | Nor. Rea. | SC. Rea. | 2SS. Rea. | Uncertainty | Counterfactual | Amount |
|-------------------|--------|-----------------|------------|------------|-------|-------|------|-----------|----------|-----------|-------------|----------------|------------|
| NuScenes-QA [49] | ✓ | ✗ | ✓ | ✓ | ✗ | ✓ | ✓ | ✗ | ✗ | ✗ | ✗ | ✗ | 460K |
| NuplanQA [48] | ✓ | ✗ | ✓ | ✓ | ✗ | ✓ | ✓ | ✗ | ✗ | ✗ | ✗ | ✗ | 1M |
| DriveLM [55] | ✓ | ✗ | ✓ | ✗ | ✗ | ✓ | ✓ | ✓ | ✗ | ✗ | ✗ | ✗ | 443K |
| DriveMLLM [21] | ✓ | ✗ | ✗ | ✗ | ✓ | ✗ | ✓ | ✗ | ✗ | ✗ | ✗ | ✗ | 4K |
| BDD-X [31] | ✓ | ✗ | ✗ | ✓ | ✓ | ✓ | ✓ | ✗ | ✗ | ✗ | ✗ | ✗ | 26K |
| DRAMA [44] | ✓ | ✗ | ✗ | ✓ | ✓ | ✓ | ✓ | ✗ | ✗ | ✗ | ✗ | ✗ | 14K |
| DriveBench [62] | ✓ | ✗ | ✓ | ✗ | ✗ | ✓ | ✓ | ✓ | ✗ | ✗ | ✗ | ✗ | 20K |
| VRU-Accident [32] | ✓ | ✓ | ✗ | ✗ | ✓ | ✓ | ✓ | ✓ | ✗ | ✗ | ✗ | ✗ | 6K |
| DVBench [68] | ✓ | ✓ | ✗ | ✗ | ✓ | ✓ | ✓ | ✓ | ✗ | ✗ | ✗ | ✗ | 10K |
| WaymoQA | ✓ | ✓ | ✓ | ✓ | ✓ | ✓ | ✓ | ✓ | ✓ | ✓ | ✓ | ✓ | 35K |

a feedback loop that reduces diversity and may even contribute to model collapse [53].

To prevent these issues and to contribute high quality data, we employ driving experts as annotators. They review selected videos and key frames and author question answer pairs as well as all MCQ options. After assembly, we conduct human verification with experts who were not involved in authoring. They solve the questions and flag issues such as excessive difficulty, ambiguous wording, or multiple plausible options. Flagged items are revised and rechecked, yielding a cleaner and more reliable benchmark. The released dataset contains **28,585** training QA pairs and **6,415** test QA pairs. A comparison with related datasets appears in Tab. 1.

4 Experiments

In this section, we evaluate a range of recent MLLMs on WaymoQA and examine the effect of fine-tuning with our training data.

4.1 Experimental Settings

We assess multiple families and sizes of state-of-the-art vision-language models and expert models, including variants of LLaVA [34, 38], InternVL [20, 60, 77], Qwen-VL [5], Phi3.5-vision [2], Gemma3 [57], and OpenDriveVLA [74]. Since Image QA and Video QA differ in both modality and question design, we separately report results for the two settings.

For **Image QA**, each example is evaluated using an eight-view input comprising front-left, front-center, front-right, side-left, side-right, rear-left, rear-center, and rear-right frames captured at the same timestamp. For **Video QA**, each video clip spans 14 seconds; due to GPU memory constraints, we uniformly sample 50 frames per video for evaluation.

4.2 Results of Image QA and Video QA.

Tabs. 2 and 3 report the performance of baselines and our fine-tuned model under the Image QA and Video QA settings across **Normal Scene**, **Others**, and **Safety-Critical** tasks. Overall, accuracy on normal scenes is relatively stable across pretrained models, whereas performance on safety-critical questions shows notable declines. Pretrained models also exhibit substantial variability and remain

well below the near-perfect human accuracy (96%) expected for this four-choice MCQ task.

In the Image QA setting (Tab. 2), Qwen2.5-VL(32B) achieves the highest overall accuracy at 65.4%, followed by Qwen2.5-VL(7B) at 62.4, while LLaVA1.5(7B) shows the lowest overall accuracy at 30.7%, only marginally above the 25% random-guess baseline. For **Others** (counterfactual and special-event questions), only Qwen2.5-VL(32B) and Gemma3(27B) exceed 60% accuracy, while all other models remain below this threshold. This pattern suggests that general-domain pretrained models do not effectively adapt to the domain-specific reasoning required in autonomous driving QA. Additionally, most models perform worse on **Safety-Critical** tasks than on **Normal Scene** understanding, indicating persistent difficulty with hazardous or risk-sensitive scenarios even with a constrained multiple-choice answer space.

In the Video QA setting (Tab. 3), safety-critical accuracy is lower than in Image QA for most models. Qwen2.5-VL(32B) attains the highest overall accuracy at 64.1%, followed by Qwen2.5-VL(7B) at 63.8%, whereas LLaVA1.5(7B) remains the weakest performer at 35.9%. Interestingly, several pretrained models obtain slightly higher accuracy on **Normal Scenes** in Video QA than in Image QA, but this does not transfer to **Safety-Critical** tasks. Only Gemma3(27B) surpasses 50% accuracy on **Safety-Critical** Video QA (51.8%), and all other models remain below this threshold, highlighting the difficulty of safety-critical reasoning over temporal context.

Fine-tuning with WaymoQA yields significant improvements across both Image QA and Video QA. For Image QA, Qwen2.5-VL(7B) increases its overall accuracy to 72.9%, corresponding to improvements of roughly **10%**, **31%**, and **17%** on **Normal Scene**, **Others**, and **Safety-Critical** tasks, respectively. For Video QA, Qwen2.5-VL(7B) rises from 63.8% to 72.8% overall accuracy, and the **Safety-Critical** accuracy improves by approximately **21%**. Notably, our WaymoQA-trained model also surpasses **GPT-5.2** on our benchmark under the same evaluation protocol (Tabs. 2 and 3). Moreover, the performance gap among task types becomes smaller after fine-tuning, indicating that WaymoQA provides targeted supervision beneficial for safety-related reasoning. Nevertheless, safety-critical

Table 2: Detailed Image QA performance of the MLLMs on WaymoQA. Bold: best; underline: second best. The following abbreviations are used: TS (Traffic Signal), SC (Scene Caption), SU (Scene Understanding), PL (Planning), PE (Perception), PR (Prediction), PP (Perception&Prediction), CF (Counterfactual), SE (Special Event), UN (Uncertainty), FT (Fine-tuning).

| Model | Normal Scene | | | | | | Others | | | Safety - Critical | | | | | | | Overall |
|--------------------------------------|--------------|-------------|-------------|-------------|-------------|-------------|-------------|-------------|-------------|-------------------|-------------|-------------|-------------|-------------|-------------|-------------|-------------|
| | TS | SC | SU | PL | PP | Overall | CF | SE | Overall | SU | PE | PR | PL | SC | UN | Overall | |
| Human Experts | 96.6 | 97.7 | 97.7 | 95.3 | 94.0 | 96.1 | 94.8 | 96.7 | 96.3 | 96.8 | 98.0 | 96.4 | 94.3 | 98.7 | 94.9 | 96.0 | 96.1 |
| GPT 5.2 | 82.0 | 88.9 | 73.1 | 71.7 | 75.4 | 75.7 | 56.4 | 57.1 | 57.0 | 68.4 | 65.6 | 73.8 | 62.3 | 57.6 | 53.0 | 64.5 | 67.4 |
| LLaVA1.5(7B) [38] | 19.6 | 24.4 | 50.0 | 24.4 | 32.8 | 35.9 | 30.7 | 39.0 | 37.5 | 24.5 | 21.3 | 24.7 | 25.5 | 27.2 | 17.0 | 23.2 | 30.7 |
| LLaVA-OneVision(7B) [34] | 71.3 | <u>78.5</u> | 73.3 | <u>65.5</u> | 56.1 | 66.7 | <u>53.6</u> | 51.4 | 51.7 | 50.8 | 42.2 | 56.9 | 53.2 | 45.5 | 64.9 | 54.4 | 58.6 |
| InternVL3.5(8B) [60] | 14.7 | 31.8 | 45.3 | 60.8 | 37.4 | 40.1 | 41.3 | 47.9 | 46.6 | 26.6 | 30.4 | 23.7 | 41.1 | 25.3 | 22.2 | 28.9 | 37.0 |
| InternVL3.5(4B) [60] | 17.6 | 32.5 | 42.5 | 43.0 | 39.6 | 38.0 | 40.2 | 42.8 | 42.3 | 21.7 | 24.1 | 23.6 | 39.2 | 41.1 | 20.2 | 27.8 | 34.4 |
| InternVL3(8B) [77] | 16.8 | 29.6 | 43.4 | 46.8 | 24.8 | 33.6 | 34.0 | 49.9 | 47.0 | 28.8 | 24.9 | 27.1 | 46.2 | 41.7 | 27.8 | 32.9 | 35.9 |
| InternVL3(14B) [77] | 20.2 | 31.2 | 45.9 | 50.0 | 39.2 | 40.2 | 42.1 | 58.6 | 55.6 | 23.4 | 32.8 | 52.1 | 45.3 | 45.8 | 39.0 | 42.1 | 44.0 |
| Qwen2.5-VL(32B) [5] | 79.9 | 81.1 | 70.7 | 64.4 | <u>69.4</u> | <u>71.2</u> | 50.0 | 62.6 | 60.3 | 52.6 | 44.6 | <u>74.3</u> | <u>64.6</u> | <u>56.4</u> | 61.4 | <u>62.6</u> | <u>65.4</u> |
| Qwen2.5-VL(7B) [5] | 77.4 | 77.4 | 71.2 | 48.4 | 63.3 | 68.1 | 43.5 | 58.9 | 55.6 | 54.4 | 55.3 | 71.0 | 64.0 | 43.0 | 54.6 | 61.1 | 62.4 |
| Phi3.5-vision [2] | 24.1 | 32.5 | 63.2 | 61.2 | 40.6 | 48.9 | 44.6 | 44.5 | 44.5 | 32.0 | 25.6 | 41.8 | 45.6 | 44.3 | 46.5 | 40.9 | 44.7 |
| Gemma3(4B) [57] | 60.2 | 62.6 | 62.6 | 56.2 | 57.1 | 59.7 | 48.0 | 48.9 | 48.7 | 34.2 | 37.1 | 53.8 | 44.3 | 51.3 | 33.8 | 43.5 | 50.6 |
| Gemma3(27B) [57] | 67.6 | 73.3 | 68.7 | 51.5 | 61.5 | 64.3 | 49.1 | <u>65.6</u> | <u>62.6</u> | <u>67.2</u> | <u>61.6</u> | 67.1 | 59.4 | 54.4 | 49.4 | 60.4 | 62.3 |
| InternVL2-DA-DriveLM(4B) [10–12, 20] | 34.0 | 58.5 | 60.2 | 66.2 | 49.6 | 54.2 | 34.6 | 38.5 | 37.7 | 44.4 | 24.1 | 41.2 | 26.8 | 38.6 | 46.1 | 36.8 | 43.6 |
| OpencodeVLA [74] | <u>82.0</u> | 76.0 | 42.1 | 50.3 | 57.1 | 54.9 | 41.3 | 44.5 | 43.9 | 57.1 | 50.7 | 68.3 | 53.1 | 41.1 | 49.6 | 56.0 | 53.4 |
| Qwen2.5-VL(7B) [5] (FT, Ours) | 84.4 | 72.6 | <u>72.0</u> | 58.5 | 80.6 | 74.9 | 63.1 | 74.8 | 72.7 | 76.1 | 76.6 | 77.8 | 65.9 | 67.8 | <u>63.8</u> | 71.2 | 72.9 |

accuracy remains well below the near-ceiling human reliability, suggesting that robust risk-sensitive understanding in driving scenes remains a major open challenge for current MLLMs.

4.3 Two-stage Consistency Evaluation.

WaymoQA formulates safety-critical reasoning as a two-stage decision process where Stage 2 is explicitly conditioned on the Stage 1 decision (Sec. 3.3).

To verify whether models truly follow this dependency, we introduce a stricter *joint correctness* evaluation. Specifically, a two-stage instance is counted as correct only if **both** Stage 1 and Stage 2 answers match the ground truth:

$$\text{Acc}_{2\text{-stage}} = \frac{1}{N} \sum_{i=1}^N \mathbb{1} \left[\hat{y}_i^{(1)} = y_i^{(1)} \wedge \hat{y}_i^{(2)} = y_i^{(2)} \right]. \quad (1)$$

As shown in Table 4, this joint evaluation causes a substantial drop for generic baselines (typically 10–20%), indicating difficulty in maintaining stage-to-stage consistency when the dependency is enforced. In contrast, models fine-tuned on WaymoQA exhibit a markedly smaller degradation, suggesting that WaymoQA supervision improves *decision-conditioned* reasoning across immediate risk resolution (Stage 1) and induced secondary risk mitigation (Stage 2).

4.4 Transfer to Planning on Waymo E2E.

Beyond QA accuracy, we examine whether WaymoQA supervision transfers to motion planning quality on the Waymo End-to-End (E2E) validation set. We report standard planning metrics including ADE at 5 seconds, where lower is better, and the robust feasibility score (RFS), where higher is better, under different training signals. As summarized in Table 5, **WaymoQA supervision alone**

improves planning performance over the baseline without additional supervision, demonstrating that learning safety-critical and risk-aware reasoning can benefit downstream driving behavior even without explicit trajectory regression. Moreover, combining WaymoQA with trajectory supervision yields the **best overall performance** and improves both ADE and RFS compared to using trajectory data alone. This suggests that WaymoQA provides complementary high-level safety-critical decision signals, while trajectory data grounds the model in geometric motion targets, and together they produce more accurate and feasible planning.

4.5 Discussion

Our results highlight a consistent limitation of pre-trained MLLMs on the WaymoQA benchmark. While these models perform competitively on normal driving scenes, they exhibit pronounced deficiencies in safety-critical scenarios. Fine-tuning on WaymoQA yields substantial gains and reduces performance disparities across task types, and it also improves accuracy on normal scenes, indicating that safety-oriented supervision can generalize beyond explicitly safety-critical cases.

We identify two recurring failure modes. First, errors in *Temporal Grounding* cause models to miss when a scene becomes safety-critical, which degrades safety-critical performance in the video domain. Second, limited understanding of relative coordinate frames, particularly instructions specified from another vehicle’s perspective, leads to mistakes in *Prediction* and *Spatial Relationship* that can propagate into unsafe *Planning*.

Beyond QA accuracy, training with WaymoQA alone improves planning metrics, and jointly training with trajectory supervision achieves the best performance, suggesting complementary benefits between high-level safety-critical decision supervision and geometric motion targets.

Table 3: Detailed Video QA performance of the MLLMs on WaymoQA. Bold: best; underline: second best. The following abbreviations are used: TS (Traffic Signal), SC (Scene Caption), SU (Scene Understanding), PL (Planning), PE (Perception), PP (Perception&Prediction), CF (Counterfactual), SE (Special Event), SR (Spatial Relationship), TG (Temporal Grounding), UN (Uncertainty), FT (Fine-tuning).

| Model | Normal Scene | | | | | Others | | | | Safety - Critical | | | | | | Overall |
|--------------------------------------|--------------|-------------|-------------|-------------|-------------|-------------|-------------|-------------|-------------|-------------------|-------------|-------------|-------------|-------------|-------------|-------------|
| | TS | SC | SU | PP | Overall | CF | SE | SR | Overall | SC | SU | PE | TG | UN | Overall | |
| Human Experts | 95.4 | 95.7 | 100.0 | 98.7 | 96.9 | 95.9 | 100.0 | 90.5 | 96.6 | 97.2 | 97.2 | 96.0 | 94.0 | 92.5 | 95.9 | 96.5 |
| GPT 5.2 | 74.0 | 70.6 | 76.3 | 85.3 | 79.1 | 82.0 | 89.4 | 47.6 | 78.8 | 54.1 | 65.5 | 50.0 | 49.0 | 81.3 | 61.6 | 72.6 |
| LLaVA1.5(7B) [38] | 26.0 | 29.4 | 48.8 | 40.4 | 42.4 | 30.0 | 40.4 | 33.3 | 34.7 | 13.5 | 27.5 | 32.6 | 27.4 | 33.3 | 27.5 | 35.9 |
| LLaVA-OneVision(7B) [34] | <u>80.0</u> | 35.2 | 68.8 | 60.7 | 65.8 | 80.0 | <u>93.6</u> | 61.9 | <u>82.1</u> | 32.4 | 43.4 | 40.3 | 29.4 | 62.5 | 42.3 | 59.2 |
| InternVL3.5(8B) [60] | 30.0 | 17.6 | 48.8 | 47.8 | 45.1 | 52.0 | 61.7 | 23.8 | 50.8 | 29.7 | 28.2 | 51.9 | 19.6 | 43.7 | 32.9 | 41.4 |
| InternVL3.5(4B) [60] | 26.0 | 41.1 | 44.1 | 28.8 | 36.3 | 62.0 | 63.8 | 38.0 | 58.4 | 37.8 | 23.4 | 42.3 | 17.6 | 39.5 | 29.3 | 36.7 |
| InternVL3(8B) [77] | 26.0 | 35.2 | 38.1 | 37.4 | 36.3 | 58.0 | 29.7 | 19.0 | 39.7 | 40.5 | 27.5 | 50.0 | 25.4 | 56.2 | 36.2 | 36.8 |
| InternVL3(14B) [77] | 28.5 | 50.0 | 51.2 | 46.0 | 46.6 | <u>72.0</u> | 60.4 | 33.3 | 60.4 | <u>59.4</u> | 27.3 | 51.9 | 25.0 | 57.4 | 38.6 | 46.3 |
| Qwen2.5-VL(32B) [5] | <u>80.0</u> | 52.9 | <u>70.6</u> | 74.2 | 72.3 | 76.6 | 93.1 | <u>57.3</u> | 79.7 | 43.2 | 46.2 | 51.9 | 31.3 | <u>67.8</u> | 47.6 | <u>64.1</u> |
| Qwen2.5-VL(7B) [5] | <u>80.0</u> | 41.1 | <u>70.6</u> | <u>76.6</u> | <u>72.7</u> | 48.0 | 89.2 | 52.3 | 64.4 | 32.4 | <u>53.1</u> | <u>55.7</u> | 31.3 | 64.5 | 49.5 | 63.8 |
| Phi3.5-vision [2] | 35.0 | 29.4 | 62.3 | 43.2 | 50.9 | 67.0 | 40.4 | 45.2 | 52.5 | 37.8 | 31.7 | 32.6 | 24.5 | 54.1 | 32.6 | 45.1 |
| Gemma3(4B) [57] | 58.0 | 52.9 | 62.3 | 58.3 | 60.0 | 70.0 | 76.6 | 33.3 | 66.1 | 54.0 | 29.6 | 38.5 | <u>54.9</u> | 54.2 | 41.1 | 53.8 |
| Gemma3(27B) [57] | 74.0 | 47.1 | 67.4 | 61.3 | 65.1 | 66.0 | 82.9 | 47.6 | 69.4 | 43.2 | 53.7 | 55.7 | 39.2 | 62.5 | <u>51.8</u> | 60.7 |
| InternVL2-DA-DriveLM(4B) [10–12, 20] | 50.0 | 70.5 | 57.2 | 57.6 | 57.0 | 36.0 | 70.2 | 52.3 | 52.5 | 37.8 | 43.4 | 30.7 | 27.4 | 58.3 | 40.5 | 50.3 |
| OpenDriveVLA [74] | 74.0 | 52.9 | 62.3 | 75.1 | 67.9 | <u>72.0</u> | 89.4 | 33.3 | 72.0 | 43.2 | 49.7 | 50.0 | 35.3 | 54.1 | 47.5 | 60.9 |
| Qwen2.5-VL(7B) [5] (FT, Ours) | 84.0 | <u>64.7</u> | 70.7 | 81.6 | 76.0 | 80.0 | 95.8 | 61.9 | 83.1 | 63.5 | 66.2 | 63.5 | 58.9 | 70.8 | 65.0 | 72.8 |

Table 4: Two-stage consistency evaluation. A prediction is correct only if both Stage 1 and Stage 2 are correct.

| Model | vanilla | 2-Stage | Δ |
|--------------------------|---------|---------|----------|
| GPT 5.2 | 67.8 | 60.9 | -6.9 |
| LlaVa-OneVision(7B) [34] | 53.0 | 38.9 | -14.1 |
| Qwen2.5-VL(32B) [5] | 65.5 | 54.6 | -10.9 |
| Gemma3(27B) [57] | 63.1 | 49.5 | -13.6 |
| OpenDriveVLA [74] | 59.3 | 52.1 | -7.2 |
| Ours | 72.8 | 70.4 | -2.4 |

Table 5: Planning performance on Waymo E2E validation split. Lower ADE is better (\downarrow) and higher RFS is better (\uparrow).

| WaymoQA | Trajectory | ADE (5s) \downarrow | RFS \uparrow |
|--------------|--------------|-----------------------|----------------|
| \times | \times | 14.3 | 5.37 |
| \checkmark | \times | 11.6 | 5.91 |
| \times | \checkmark | 4.23 | 6.37 |
| \checkmark | \checkmark | 3.81 | 6.91 |

WaymoQA provides scene-complete human annotations for safety-critical scenarios. Restructuring these annotations into supervision that directly targets temporal risk localization and agent-centric reasoning may mitigate the above failure modes, and it may further support future evaluation of higher-order safety-critical reasoning beyond the current setting.

5 Conclusion

We introduced WaymoQA, a multi view driving QA dataset centered on safety-critical reasoning, with 28,585 train and 6,415 test set across video and image. It defines Safety-Critical Reasoning as a two stage task and provides human annotated four option MCQ evaluation. Our experiments show that recent MLLMs underperform on safety-critical scenes compared to normal scenes, but the model fine-tuned on WaymoQA largely closes this gap. Results highlight the importance of targeted supervision on safety-critical multi view data and position WaymoQA as a foundation for future work on various tasks in safety-critical driving.

References

- [1] Ahmed S Abdelrahman, Mohamed Abdel-Aty, and Dongdong Wang. 2025. Video-to-text pedestrian monitoring (vtpm): Leveraging large language models for privacy-preserve pedestrian activity monitoring at intersections. In *Proceedings of the Winter Conference on Applications of Computer Vision*. 366–375.
- [2] Marah Abdin, Jyoti Aneja, Hany Awadalla, Ahmed Awadallah, Ammar Ahmad Awan, Nguyen Bach, Amit Bahree, Arash Bakhtiari, Jianmin Bao, Harkirat Behl, Alon Benhaim, Misha Bilenko, Johan Bjorck, Sébastien Bubeck, Martin Cai, Qin Cai, Vishrav Chaudhary, Dong Chen, Dongdong Chen, Weizhu Chen, Yen-Chun Chen, Yi-Ling Chen, Hao Cheng, Parul Chopra, Xiyang Dai, Matthew Dixon, Ronen Eldan, Victor Fragoso, Jianfeng Gao, Mei Gao, Min Gao, Amit Garg, Allie Del Giorno, Abhishek Goswami, Suriya Gunasekar, Emman Haider, Junheng Hao, Russell J. Hewett, Wenxiang Hu, Jamie Huynh, Dan Iter, Sam Ade Jacobs, Mojan Javaheripi, Xin Jin, Nikos Karampatziaakis, Piero Kauffmann, Mahoud Khademi, Dongwoo Kim, Young Jin Kim, Lev Kurilenko, James R. Lee, Yin Tat Lee, Yanzhi Li, Yunsheng Li, Chen Liang, Lars Liden, Xihui Lin, Zeqi Lin, Ce Liu, Liyuan Liu, Mengchen Liu, Weishung Liu, Xiaodong Liu, Chong Luo, Piyush Madan, Ali Mahmoudzadeh, David Majercak, Matt Mazzola, Caio César Teodoro Mendes, Arindam Mitra, Hardik Modi, Anh Nguyen, Brandon Norick, Barun Patra, Daniel Perez-Becker, Thomas Portet, Reid Pryzant, Heyang Qin, Marko Radmilac, Liliang Ren, Gustavo de Rosa, Corby Rosset, Sambudha Roy, Olatunji Ruwase, Olli Saarikivi, Amin Saied, Adil Salim, Michael Santacroce, Shital Shah, Ning Shang, Hiteshi Sharma, Yelong Shen, Swadheen Shukla, Xia Song, Masahiro Tanaka, Andrea Tupini, Praneetha Vaddamanu, Chunyu Wang, Guanhua Wang, Lijuan Wang, Shuohang Wang, Xin Wang, Yu Wang, Rachel Ward, Wen Wen, Philipp Witte, Haiping Wu, Xiaoxia Wu, Michael Wyatt, Bin Xiao, Can Xu, Jiahang Xu,

- Weijian Xu, Jilong Xue, Sonali Yadav, Fan Yang, Jianwei Yang, Yifan Yang, Ziyi Yang, Donghan Yu, Lu Yuan, Chenruidong Zhang, Cyril Zhang, Jianwen Zhang, Li Lina Zhang, Yi Zhang, Yue Zhang, Yunan Zhang, and Xiren Zhou. 2024. Phi-3 Technical Report: A Highly Capable Language Model Locally on Your Phone. arXiv:2404.14219 [cs.CL] <https://arxiv.org/abs/2404.14219>
- [3] National Highway Traffic Safety Administration et al. 2007. Pre-crash scenario typology for crash avoidance research. *DOT HS 810 (2007)*, 767.
- [4] Aishwarya Agrawal, Dhruv Batra, Devi Parikh, and Aniruddha Kembhavi. 2018. Don't just assume; look and answer: Overcoming priors for visual question answering. In *Proceedings of the IEEE conference on computer vision and pattern recognition*. 4971–4980.
- [5] Shuai Bai, Keqin Chen, Xuejing Liu, Jialin Wang, Wenbin Ge, Sibao Song, Kai Dang, Peng Wang, Shijie Wang, Jun Tang, et al. 2025. Qwen2.5-vl technical report. *arXiv preprint arXiv:2502.13923 (2025)*.
- [6] Boyuan Chen, Zhuo Xu, Sean Kirmani, Brain Ichter, Dorsa Sadigh, Leonidas Guibas, and Fei Xia. 2024. Spatialvlm: Endowing vision-language models with spatial reasoning capabilities. In *Proceedings of the IEEE/CVF Conference on Computer Vision and Pattern Recognition*. 14455–14465.
- [7] Dongping Chen, Ruoxi Chen, Shilin Zhang, Yaochen Wang, Yinyu Liu, Huichi Zhou, Qihui Zhang, Yao Wan, Pan Zhou, and Lichao Sun. 2024. Mllm-as-a-judge: Assessing multimodal llm-as-a-judge with vision-language benchmark. In *Forty-first International Conference on Machine Learning*.
- [8] Long Chen, Oleg Sinavski, Jan Hünermann, Alice Karnsund, Andrew James Willmott, Danny Birch, Daniel Maund, and Jamie Shotton. 2024. Driving with llms: Fusing object-level vector modality for explainable autonomous driving. In *2024 IEEE International Conference on Robotics and Automation (ICRA)*. IEEE, 14093–14100.
- [9] Wei-Lin Chen, Zhepei Wei, Xinyu Zhu, Shi Feng, and Yu Meng. [n. d.]. Do llm evaluators prefer themselves for a reason?. 2025. URL <https://arxiv.org/abs/2504.03846> 2504 (n. d.).
- [10] Zhe Chen, Weiyun Wang, Yue Cao, Yangzhou Liu, Zhangwei Gao, Erfei Cui, Jinguo Zhu, Shenglong Ye, Hao Tian, Zhaoyang Liu, et al. 2024. Expanding Performance Boundaries of Open-Source Multimodal Models with Model, Data, and Test-Time Scaling. *arXiv preprint arXiv:2412.05271 (2024)*.
- [11] Zhe Chen, Weiyun Wang, Hao Tian, Shenglong Ye, Zhangwei Gao, Erfei Cui, Wenwen Tong, Kongzhi Hu, Jiapeng Luo, Zheng Ma, et al. 2024. How Far Are We to GPT-4V? Closing the Gap to Commercial Multimodal Models with Open-Source Suites. *arXiv preprint arXiv:2404.16821 (2024)*.
- [12] Zhe Chen, Jiannan Wu, Wenhai Wang, Weijie Su, Guo Chen, Sen Xing, Muyan Zhong, Qinglong Zhang, Xizhou Zhu, Lewei Lu, et al. 2024. Internvl: Scaling up vision foundation models and aligning for generic visual-linguistic tasks. In *Proceedings of the IEEE/CVF Conference on Computer Vision and Pattern Recognition*. 24185–24198.
- [13] Can Cui, Yunsheng Ma, Xu Cao, Wenqian Ye, and Ziran Wang. 2024. Drive as you speak: Enabling human-like interaction with large language models in autonomous vehicles. In *Proceedings of the IEEE/CVF Winter Conference on Applications of Computer Vision*. 902–909.
- [14] Xinpeng Ding, Jianhua Han, Hang Xu, Wei Zhang, and Xiaomeng Li. 2025. HiLM-D: Enhancing MLLMs with Multi-scale High-Resolution Details for Autonomous Driving. *International Journal of Computer Vision (2025)*, 1–17.
- [15] Alexey Dosovitskiy, German Ros, Felipe Codevilla, Antonio Lopez, and Vladlen Koltun. 2017. CARLA: An open urban driving simulator. In *Conference on robot learning*. PMLR, 1–16.
- [16] Jianwu Fang, Lei-lei Li, Junfei Zhou, Junbin Xiao, Hongkai Yu, Chen Lv, Jianru Xue, and Tat-Seng Chua. 2024. Abductive ego-view accident video understanding for safe driving perception. In *Proceedings of the IEEE/CVF Conference on Computer Vision and Pattern Recognition*. 22030–22040.
- [17] Bowen Feng, Zhiting Mei, Baiang Li, Julian Ost, Roger Girgis, Anirudha Majumdar, and Felix Heide. 2025. VERDI: VLM-Embedded Reasoning for Autonomous Driving. *arXiv preprint arXiv:2505.15925 (2025)*.
- [18] Chaoyou Fu, Yuhang Dai, Yongdong Luo, Lei Li, Shuhuai Ren, Renrui Zhang, Zihan Wang, Chenyu Zhou, Yunhang Shen, Mengdan Zhang, et al. 2025. Video-mme: The first-ever comprehensive evaluation benchmark of multi-modal llms in video analysis. In *Proceedings of the Computer Vision and Pattern Recognition Conference*. 24108–24118.
- [19] Daocheng Fu, Xin Li, Licheng Wen, Min Dou, Pinlong Cai, Botian Shi, and Yu Qiao. 2024. Drive like a human: Rethinking autonomous driving with large language models. In *2024 IEEE/CVF Winter Conference on Applications of Computer Vision Workshops (WACVW)*. IEEE, 910–919.
- [20] Zhangwei Gao, Zhe Chen, Erfei Cui, Yiming Ren, Weiyun Wang, Jinguo Zhu, Hao Tian, Shenglong Ye, Junjun He, Xizhou Zhu, et al. 2024. Mini-internvl: A flexible-transfer pocket multimodal model with 5% parameters and 90% performance. *arXiv preprint arXiv:2410.16261 (2024)*.
- [21] Xianda Guo, Ruijun Zhang, Yiqun Duan, Yuhang He, Chenming Zhang, Shuai Liu, and Long Chen. 2024. Drivemllm: A benchmark for spatial understanding with multimodal large language models in autonomous driving. *arXiv e-prints (2024)*, arXiv–2411.
- [22] Ziang Guo, Konstantin Gubernatorov, Selamawit Asfaw, Zakhar Yagudin, and Dzmitry Tsetserukou. 2025. Vdt-auto: End-to-end autonomous driving with vlm-guided diffusion transformers. *arXiv preprint arXiv:2502.20108 (2025)*.
- [23] Wencheng Han, Dongqian Guo, Cheng-Zhong Xu, and Jianbing Shen. 2025. Dme-driver: Integrating human decision logic and 3d scene perception in autonomous driving. In *Proceedings of the AAAI Conference on Artificial Intelligence*, Vol. 39. 3347–3355.
- [24] Wenyi Hong, Weihang Wang, Qingsong Lv, Jiazheng Xu, Wenmeng Yu, Junhui Ji, Yan Wang, Zihan Wang, Yuxiao Dong, Ming Ding, et al. 2024. Cogagent: A visual language model for gui agents. In *Proceedings of the IEEE/CVF Conference on Computer Vision and Pattern Recognition*. 14281–14290.
- [25] Anthony Hu, Lloyd Russell, Hudson Yeo, Zak Murez, George Fedoseev, Alex Kendall, Jamie Shotton, and Gianluca Corrado. 2023. Gaia-1: A generative world model for autonomous driving. *arXiv preprint arXiv:2309.17080 (2023)*.
- [26] Zhijian Huang, Tao Tang, Shaoxiang Chen, Sihao Lin, Zequn Jie, Lin Ma, Guanrun Wang, and Xiaodan Liang. 2024. Making large language models better planners with reasoning-decision alignment. In *European Conference on Computer Vision*. Springer, 73–90.
- [27] Jyh-Jing Hwang, Runsheng Xu, Hubert Lin, Wei-Chih Hung, Jingwei Ji, Kristy Choi, Di Huang, Tong He, Paul Covington, Benjamin Sapp, et al. 2024. Emma: End-to-end multimodal model for autonomous driving. *arXiv preprint arXiv:2410.23262 (2024)*.
- [28] Ye Jin, Ruoxuan Yang, Zhijie Yi, Xiaoxi Shen, Huiling Peng, Xiaolan Liu, Jingli Qin, Jiayang Li, Jintao Xie, Peizhong Gao, et al. 2024. Surrealdriver: Designing llm-powered generative driver agent framework based on human drivers' driving-thinking data. In *2024 IEEE/RSJ International Conference on Intelligent Robots and Systems (IROS)*. IEEE, 966–971.
- [29] Justin Johnson, Bharath Hariharan, Laurens Van Der Maaten, Li Fei-Fei, C Lawrence Zitnick, and Ross Girshick. 2017. Clevr: A diagnostic dataset for compositional language and elementary visual reasoning. In *Proceedings of the IEEE conference on computer vision and pattern recognition*. 2901–2910.
- [30] Boshra Khalili and Andrew W Smyth. 2025. Autodrive-qa-automated generation of multiple-choice questions for autonomous driving datasets using large vision-language models. *arXiv preprint arXiv:2503.15778 (2025)*.
- [31] Jinkyu Kim, Anna Rohrbach, Trevor Darrell, John Canny, and Zeynep Akata. 2018. Textual explanations for self-driving vehicles. In *Proceedings of the European conference on computer vision (ECCV)*. 563–578.
- [32] Yunggun Kim, Ahmed S Abdelrahman, and Mohamed Abdel-Aty. 2025. VRU-Accident: A Vision-Language Benchmark for Video Question Answering and Dense Captioning for Accident Scene Understanding. In *Proceedings of the IEEE/CVF International Conference on Computer Vision*. 761–771.
- [33] Yuwon Lee. 2024. Qwen2-VL-Finetune. <https://github.com/2U1/Qwen2-VL-Finetune>
- [34] Bo Li, Yuanhan Zhang, Dong Guo, Renrui Zhang, Feng Li, Hao Zhang, Kaichen Zhang, Peiyuan Zhang, Yanwei Li, Ziwei Liu, et al. 2024. Llava-onevision: Easy visual task transfer. *arXiv preprint arXiv:2408.03326 (2024)*.
- [35] Cheng Li, Keyuan Zhou, Tong Liu, Yu Wang, Mingqiao Zhuang, Huan-ang Gao, Bu Jin, and Hao Zhao. 2025. Avid2: Accident video diffusion for accident video description. *arXiv preprint arXiv:2502.14801 (2025)*.
- [36] Kunchang Li, Yali Wang, Yinan He, Yizhuo Li, Yi Wang, Yi Liu, Zun Wang, Jilan Xu, Guo Chen, Ping Luo, et al. 2024. Mvbench: A comprehensive multi-modal video understanding benchmark. In *Proceedings of the IEEE/CVF Conference on Computer Vision and Pattern Recognition*. 22195–22206.
- [37] Haohong Lin, Xin Huang, Tung Phan, David Hayden, Huan Zhang, Ding Zhao, Siddhartha Srinivasa, Eric Wolff, and Hongge Chen. 2025. Causal composition diffusion model for closed-loop traffic generation. In *Proceedings of the Computer Vision and Pattern Recognition Conference*. 27542–27552.
- [38] Haotian Liu, Chunyuan Li, Yuheng Li, and Yong Jae Lee. 2024. Improved baselines with visual instruction tuning. In *Proceedings of the IEEE/CVF conference on computer vision and pattern recognition*. 26296–26306.
- [39] Haolan Liu, Liangjun Zhang, Siva Kumar Sastry Hari, and Jishen Zhao. 2024. Safety-critical scenario generation via reinforcement learning based editing. In *2024 IEEE International Conference on Robotics and Automation (ICRA)*. IEEE, 14405–14412.
- [40] Yuan Liu, Haodong Duan, Yuanhan Zhang, Bo Li, Songyang Zhang, Wangbo Zhao, Yike Yuan, Jiaqi Wang, Conghui He, Ziwei Liu, et al. 2024. Mmbench: Is your multi-modal model an all-around player?. In *European conference on computer vision*. Springer, 216–233.
- [41] Zuyan Liu, Yuhao Dong, Yongming Rao, Jie Zhou, and Jiwen Lu. 2024. Chain-of-spot: Interactive reasoning improves large vision-language models. *arXiv preprint arXiv:2403.12966 (2024)*.
- [42] Haohan Luo and Feng Wang. 2023. A simulation-based framework for urban traffic accident detection. In *ICASSP 2023-2023 IEEE International Conference on Acoustics, Speech and Signal Processing (ICASSP)*. IEEE, 1–5.
- [43] Yingzi Ma, Yulong Cao, Jiachen Sun, Marco Pavone, and Chaowei Xiao. 2024. Dolphins: Multimodal language model for driving. In *European Conference on Computer Vision*. Springer, 403–420.

- [44] Srikanth Malla, Chiho Choi, Isht Dwivedi, Joon Hee Choi, and Jiachen Li. 2023. Drama: Joint risk localization and captioning in driving. In *Proceedings of the IEEE/CVF winter conference on applications of computer vision*. 1043–1052.
- [45] Jiageng Mao, Yuxi Qian, Junjie Ye, Hang Zhao, and Yue Wang. 2023. Gpt-driver: Learning to drive with gpt. *arXiv preprint arXiv:2310.01415* (2023).
- [46] Kenneth Marino, Mohammad Rastegari, Ali Farhadi, and Roozbeh Mottaghi. 2019. Ok-vqa: A visual question answering benchmark requiring external knowledge. In *Proceedings of the IEEE/cvf conference on computer vision and pattern recognition*. 3195–3204.
- [47] Chirag Parikh, Deepti Rawat, Tathagata Ghosh, Ravi Kiran Sarvadevabhatla, et al. 2025. RoadSocial: A Diverse VideoQA Dataset and Benchmark for Road Event Understanding from Social Video Narratives. In *Proceedings of the Computer Vision and Pattern Recognition Conference*. 19002–19011.
- [48] Sung-Yeon Park, Can Cui, Yunsheng Ma, Ahmadreza Moradipari, Rohit Gupta, Kyungtae Han, and Ziran Wang. 2025. NuPlanqa: A large-scale dataset and benchmark for multi-view driving scene understanding in multi-modal large language models. *arXiv preprint arXiv:2503.12772* (2025).
- [49] Tianwen Qian, Jingjing Chen, Linhai Zhuo, Yang Jiao, and Yu-Gang Jiang. 2024. Nuscenes-qa: A multi-modal visual question answering benchmark for autonomous driving scenario. In *Proceedings of the AAAI Conference on Artificial Intelligence*, Vol. 38. 4542–4550.
- [50] Davis Rempe, Jonah Philion, Leonidas J Guibas, Sanja Fidler, and Or Litany. 2022. Generating useful accident-prone driving scenarios via a learned traffic prior. In *Proceedings of the IEEE/CVF Conference on Computer Vision and Pattern Recognition*. 17305–17315.
- [51] Hao Shao, Yuxuan Hu, Letian Wang, Guanglu Song, Steven L Waslander, Yu Liu, and Hongsheng Li. 2024. Lmndrive: Closed-loop end-to-end driving with large language models. In *Proceedings of the IEEE/CVF Conference on Computer Vision and Pattern Recognition*. 15120–15130.
- [52] Zhihong Shao, Peiyi Wang, Qihao Zhu, Runxin Xu, Junxiao Song, Xiao Bi, Haowei Zhang, Mingchuan Zhang, YK Li, Yang Wu, et al. 2024. Deepseekmath: Pushing the limits of mathematical reasoning in open language models. *arXiv preprint arXiv:2402.03300* (2024).
- [53] Ilya Shumailov, Zakhar Shumaylov, Yiren Zhao, Nicolas Papernot, Ross Anderson, and Yarín Gal. 2024. AI models collapse when trained on recursively generated data. *Nature* 631, 8022 (2024), 755–759.
- [54] Chonghao Sima, Kashyap Chitta, Zhiding Yu, Shiyi Lan, Ping Luo, Andreas Geiger, Hongyang Li, and Jose M Alvarez. 2025. Centaur: Robust end-to-end autonomous driving with test-time training. *arXiv preprint arXiv:2503.11650* (2025).
- [55] Chonghao Sima, Katrin Renz, Kashyap Chitta, Li Chen, Hanxue Zhang, Chengen Xie, Jens Beißwenger, Ping Luo, Andreas Geiger, and Hongyang Li. 2024. Drivelm: Driving with graph visual question answering. In *European conference on computer vision*. Springer, 256–274.
- [56] Austin Stone, Ted Xiao, Yao Lu, Keerthana Gopalakrishnan, Kuang-Huei Lee, Quan Vuong, Paul Wohlhart, Sean Kirmani, Brianna Zitkovich, Fei Xia, et al. 2023. Open-world object manipulation using pre-trained vision-language models. *arXiv preprint arXiv:2303.00905* (2023).
- [57] Gemma Team, Aishwarya Kamath, Johan Ferret, Shreya Pathak, Nino Vieillard, Ramona Merhej, Sarah Perrin, Tatiana Matejovicova, Alexandre Ramé, Morgane Rivière, et al. 2025. Gemma 3 technical report. *arXiv preprint arXiv:2503.19786* (2025).
- [58] Xiaoyu Tian, Junru Gu, Bailin Li, Yicheng Liu, Yang Wang, Zhiyong Zhao, Kun Zhan, Peng Jia, Xianpeng Lang, and Hang Zhao. 2024. Drivelm: The convergence of autonomous driving and large vision-language models. *arXiv preprint arXiv:2402.12289* (2024).
- [59] Tianqi Wang, Sukmin Kim, Ji Wenxuan, Enze Xie, Chongjian Ge, Junsong Chen, Zhenguo Li, and Ping Luo. 2024. Deepaccident: A motion and accident prediction benchmark for v2x autonomous driving. In *Proceedings of the AAAI Conference on Artificial Intelligence*, Vol. 38. 5599–5606.
- [60] Weiyun Wang, Zhangwei Gao, Lixin Gu, Hengjun Pu, Long Cui, Xingguang Wei, Zhaoyang Liu, Linglin Jing, Shenglong Ye, Jie Shao, et al. 2025. Internvl3. 5: Advancing open-source multimodal models in versatility, reasoning, and efficiency. *arXiv preprint arXiv:2508.18265* (2025).
- [61] Koki Wataoka, Tsubasa Takahashi, and Ryokan Ri. 2024. Self-preference bias in llm-as-a-judge. *arXiv preprint arXiv:2410.21819* (2024).
- [62] Shaoyuan Xie, Lingdong Kong, Yuhao Dong, Chonghao Sima, Wenwei Zhang, Qi Alfred Chen, Ziwei Liu, and Liang Pan. 2025. Are vlms ready for autonomous driving? an empirical study from the reliability, data, and metric perspectives. *arXiv preprint arXiv:2501.04003* (2025).
- [63] Yuting Xie, Xianda Guo, Cong Wang, Kunhua Liu, and Long Chen. [n. d.]. Advdiffuser: Generating adversarial safety-critical driving scenarios via guided diffusion. In 2024 IEEE. In *RSJ International Conference on Intelligent Robots and Systems (IROS)*. 9983–9989.
- [64] Runsheng Xu, Hubert Lin, Wonseok Jeon, Hao Feng, Yuliang Zou, Liting Sun, John Gorman, Kate Tolstaya, Sarah Tang, Brandyn White, et al. 2025. WOD-E2E: Waymo Open Dataset for End-to-End Driving in Challenging Long-tail Scenarios. *arXiv preprint arXiv:2510.26125* (2025).
- [65] Zhenhua Xu, Yujia Zhang, Enze Xie, Zhen Zhao, Yong Guo, Kwan-Yee K Wong, Zhenguo Li, and Hengshuang Zhao. 2024. Drivegpt4: Interpretable end-to-end autonomous driving via large language model. *IEEE Robotics and Automation Letters* (2024).
- [66] Yu Yao, Xizi Wang, Mingze Xu, Zelin Pu, Yuchen Wang, Ella Atkins, and David J Crandall. 2022. DoTA: Unsupervised detection of traffic anomaly in driving videos. *IEEE transactions on pattern analysis and machine intelligence* 45, 1 (2022), 444–459.
- [67] Haoxuan You, Haotian Zhang, Zhe Gan, Xianzhi Du, Bowen Zhang, Zirui Wang, Liangliang Cao, Shih-Fu Chang, and Yinfei Yang. 2023. Ferret: Refer and ground anything anywhere at any granularity. *arXiv preprint arXiv:2310.07704* (2023).
- [68] Tong Zeng, Longfeng Wu, Liang Shi, Dawei Zhou, and Feng Guo. 2025. Are vision llms road-ready? a comprehensive benchmark for safety-critical driving video understanding. In *Proceedings of the 31st ACM SIGKDD Conference on Knowledge Discovery and Data Mining V. 2*. 5972–5983.
- [69] Jiawei Zhang, Chejian Xu, and Bo Li. 2024. Chatscene: Knowledge-enabled safety-critical scenario generation for autonomous vehicles. In *Proceedings of the IEEE/CVF Conference on Computer Vision and Pattern Recognition*. 15459–15469.
- [70] Zangwei Zheng, Xiangyu Peng, Tianji Yang, Chenhui Shen, Shenggui Li, Hongxin Liu, Yukun Zhou, Tianyi Li, and Yang You. 2024. Open-sora: Democratizing efficient video production for all. *arXiv preprint arXiv:2412.20404* (2024).
- [71] Ziyuan Zhong, Davis Rempe, Yuxiao Chen, Boris Ivanovic, Yulong Cao, Danfei Xu, Marco Pavone, and Baishakhi Ray. 2023. Language-guided traffic simulation via scene-level diffusion. In *Conference on robot learning*. PMLR, 144–177.
- [72] Ziyuan Zhong, Davis Rempe, Danfei Xu, Yuxiao Chen, Sushant Veer, Tong Che, Baishakhi Ray, and Marco Pavone. 2022. Guided conditional diffusion for controllable traffic simulation. *arXiv preprint arXiv:2210.17366* (2022).
- [73] Jiawei Zhou, Linye Lyu, Zhuotao Tian, Cheng Zhuo, and Yu Li. 2025. SafeMV-Drive: Multi-view Safety-Critical Driving Video Synthesis in the Real World Domain. *arXiv preprint arXiv:2505.17727* (2025).
- [74] Xingcheng Zhou, Xuyuan Han, Feng Yang, Yunpu Ma, and Alois C Knoll. 2025. Opendrivevla: Towards end-to-end autonomous driving with large vision language action model. *arXiv preprint arXiv:2503.23463* (2025).
- [75] Zewei Zhou, Tianhui Cai, Seth Z Zhao, Yun Zhang, Zhiyu Huang, Bolei Zhou, and Jiaqi Ma. 2025. AutoVLA: A Vision-Language-Action Model for End-to-End Autonomous Driving with Adaptive Reasoning and Reinforcement Fine-Tuning. *arXiv preprint arXiv:2506.13757* (2025).
- [76] Deyao Zhu, Jun Chen, Xiaoqian Shen, Xiang Li, and Mohamed Elhoseiny. 2023. Minigt-4: Enhancing vision-language understanding with advanced large language models. *arXiv preprint arXiv:2304.10592* (2023).
- [77] Jinguo Zhu, Weiyun Wang, Zhe Chen, Zhaoyang Liu, Shenglong Ye, Lixin Gu, Hao Tian, Yuchen Duan, Weijie Su, Jie Shao, et al. 2025. Internvl3: Exploring advanced training and test-time recipes for open-source multimodal models. *arXiv preprint arXiv:2504.10479* (2025).

A Fine-Tuning and Implementation Details

A.1 Fine-Tuning Details

We fine-tune Qwen2.5 VL(7B) following the official guideline [33]. The base weights of the language and vision towers and the projector are frozen, and LoRA adapters are applied to all supported modules except the LM head and token embeddings. The batch size is 32 and learning rate is $2e-4$. For data construction, videos are packed with all QA pairs associated with the clip and key frames are packed with all QA pairs anchored to the frame.

For training stability, we sample video at 1.2 FPS and train with a multi image fine tuning setup analogous to Image QA. Video data consist of 22 second multi view clips that impose substantial memory demand; accordingly, we use 1.2 FPS under the available hardware constraints. We expect non-uniform sampling to improve learning by allocating samples to key frames and fewer to less informative frames. In practice the 28,585 training pool benefited from allocating at least 20,000 examples to training. Validation sets larger than 8,000 were associated with lower accuracy.

A.2 Implementation Details

We fine-tune Qwen2.5-VL-7B-Instruct on WaymoQA using 8×NVIDIA RTX A6000 GPUs with DeepSpeed ZeRO-2. We adopt parameter-efficient fine-tuning with LoRA following the official guideline [33]. Both language and vision modules are equipped with LoRA adapters (rank 64, $\alpha = 64$, dropout 0.05), while the base vision tower, language model, and merger module are frozen. Following the official Qwen2.5-VL setup, we exclude the token embedding and output head from LoRA (`lm_head`, `embed_tokens`) and keep all other linear layers trainable through adapters. We enable Liger kernels for efficient attention, gradient checkpointing for memory savings, and train in `bf16` with `tf32` enabled on matrix multiplications.

Training uses a global batch size of 32 (per-device batch size 1 on 8 GPUs with gradient accumulation of 4), for 3 epochs over the WaymoQA training split. We apply a cosine learning rate schedule with an initial learning rate of 2×10^{-4} , a warm-up ratio of 0.03, and weight decay of 0.1. Images are dynamically resized within the range of $256 \times 28 \times 28$ to $1024 \times 28 \times 28$ pixels to balance resolution and memory usage.

B Question Categories and Statistics

Table 6 summarizes how the 62-item question bank is instantiated across **Format** (Image / Video), **Scene type** (Normal / Safety-critical / Others), and **Task** categories.

Table 6: Distribution of questions in WaymoQA by format, scene type, and task category.

| Type | Scene | Category | Count |
|------------|-----------------|-------------------------------------|---------------|
| Image | Normal | Normal Perception & Prediction | 4,004 |
| Image | Normal | Normal Planning | 1,518 |
| Image | Normal | Normal scene Understanding | 4,606 |
| Image | Normal | Normal scene caption | 1,134 |
| Image | Normal | Traffic Signal | 1,266 |
| Image | Others | Counterfactual | 1,616 |
| Image | Others | Spatial Relationship | 351 |
| Image | Others | Special Event | 1,927 |
| Image | Safety-critical | Safety-critical Perception | 1,375 |
| Image | Safety-critical | Safety-critical Planning | 3,239 |
| Image | Safety-critical | Safety-critical Prediction | 2,990 |
| Image | Safety-critical | Safety-critical scene Understanding | 1,926 |
| Image | Safety-critical | Safety-critical scene caption | 1,060 |
| Image | Safety-critical | Uncertainty | 2,317 |
| Video | Normal | Normal Perception & Prediction | 1,080 |
| Video | Normal | Normal scene Understanding | 1,270 |
| Video | Normal | Normal scene caption | 290 |
| Video | Normal | Traffic Signal | 300 |
| Video | Others | Counterfactual | 316 |
| Video | Others | Spatial Relationship | 143 |
| Video | Others | Special Event | 202 |
| Video | Safety-critical | Safety-critical Perception | 324 |
| Video | Safety-critical | Safety-critical scene Understanding | 874 |
| Video | Safety-critical | Safety-critical scene caption | 290 |
| Video | Safety-critical | Temporal Grounding | 316 |
| Video | Safety-critical | Uncertainty | 288 |
| Sum | | | 35,022 |

Task definitions. Below we briefly describe each reasoning category covered by the question bank.

Caption. These questions ask the model to produce or select a caption summarizing the scene. For *normal* scenes, the caption

focuses on overall driving context such as road layout, traffic participants, and general situation. For *safety critical* scenes, the caption is required to highlight the safety relevant situation, such as an imminent collision risk or a blocked lane.

Scene Understanding. Compared to Caption, these questions probe more fine grained comprehension of the scene. They query specific aspects of the environment such as which lanes are drivable, who has right of way, and where the ego vehicle is positioned rather than a single high level summary.

Perception. Perception questions ask about properties or states of objects in the scene: their type such as car, pedestrian, cyclist, or construction vehicle, their attributes such as parked or moving or indicating, and their positions relative to the ego vehicle or road structure.

Prediction. Prediction questions require anticipating the *future behavior* of agents. Typical queries include whether another vehicle will cut in, whether a pedestrian is likely to cross, or how surrounding traffic will evolve in the next few seconds.

Planning. Planning questions focus on the ego vehicle’s *future action*. The model must decide an appropriate maneuver such as continue, slow down, stop, or change lanes, given the perceived scene and expected motions of other agents.

Uncertainty. These questions target reasoning about unknown or unobserved risk, such as occluded areas, blind spots, or partially visible agents. The model must recognize where it cannot be certain, for example when a pedestrian may emerge from behind a truck, and reflect this uncertainty in its choice.

Counterfactual. Counterfactual questions describe hypothetical deviations from the current situation. They typically ask what would happen *if* the ego vehicle or another agent took a different action, for example what would likely occur if the ego vehicle changed lanes now, probing causal reasoning about alternative behaviors.

Special Event. Special Event questions focus on unusual but practically important conditions, such as road construction, emergency vehicles, accidents, or adverse weather such as rain, snow, or poor visibility. The model must detect these events and understand their impact on safe driving.

Spatial Relationship. These questions query the interaction and relative positioning between two or more objects. Examples include determining which vehicle is ahead or behind, which lane another car occupies, or whether two agents are on a collision course.

Temporal Grounding. Temporal Grounding questions ask *when* in a video the situation becomes safety critical. The model must identify the time interval or frame range where risk emerges or peaks, rather than only describing a single static frame, and this category is defined for video data only.

Table 7: Representative question templates for each reasoning category in the WaymoQA question bank.

| Category | Representative question templates |
|-------------------------------------|--|
| Normal Prediction & Planning | Based on the current appearance of the person or two-wheeled vehicle, how do they intend to move? Which of the following describes a non-safety-critical object? |
| Normal Planning | What actions are currently available? |
| Normal Scene Understanding | Which of the following statements about traffic density is correct? How is the behavior of the vehicle summarized before the event? |
| Normal Scene Caption | Which of the following is correct as an image caption from the perspective of a normal frame? What is the video summary from the perspective of a normal scene? |
| Counterfactual | What situation might occur if the vehicle acted this way? What are the potential situations that could occur in the current scenario? |
| Spatial Relationship | What is the spatial relationship of two or more objects? |
| Special Event | Is there a special situation? What are the restrictions on behavior in school zones or congested areas? What is the plan for yielding when an ambulance or fire truck approaches? |
| Safety-critical Perception | What is a safety-critical object? |
| Safety-critical Planning | What are the driving guidelines for the ego vehicle based on the behavior of safety-critical objects? How should the ego vehicle drive to solve the first hazard while also addressing the second hazard? |
| Safety-critical Prediction | How do you think a safety-critical object will move? Are there any other safety-critical objects besides the first safety-critical object? If so, how would they move? |
| Safety-critical Scene Understanding | What is the correlation in safety-critical situations? How did the safety-critical object move and how did the ego vehicle behave? |
| Safety-critical Scene Caption | What is the correct image caption from the perspective of a safety-critical frame? What is correct regarding video summary from a safety-critical scene perspective? |
| Uncertainty | Where is the area that hides the danger in the current frame? Is there a blind spot in the field of view? |
| Temporal Grounding | Where is the safety-critical situation in the video? |
| Traffic Signal | Which of the following is a correct description of traffic signals? |

Traffic Signal. These questions assess correct interpretation of traffic lights, arrows, and lane markings and how they constrain ego behavior. They often require relating signal state such as red light, protected left arrow, or lane only sign to valid or invalid driving actions.

We further provide representative question templates for each reasoning category in Table 7.

C Criteria of Converting Annotation into MCQ

In order to construct the multiple-choice questions (MCQ) used in WaymoQA, we convert human-annotated answers into a structured four-choice format. Each MCQ requires one correct answer and three plausible false candidates. The false answers must be carefully designed so that the overall difficulty remains appropriate. Our target difficulty range ensures that pretrained models score roughly between 30% and 70% because scores below 30% indicate that the question is unnecessarily difficult, and scores above 70% mean that the question is too easy. We iteratively refine the criteria by creating subsets of MCQs, and adjusting the false-choices construction rules. The final criteria are summarized below.

1. The question must not be solvable from text input alone.

False choices that are irrelevant, exaggerated, or logically disconnected allow models to answer correctly without looking at the image. To avoid this issue, all candidates must remain close to the topic of the question. Each false answer should carry plausible content that resembles the correct answer so that visual understanding is required.

2. False choices must be visually similar to the correct answer.

To ensure that the MCQ reflects genuine visual reasoning, false candidates must be close variants of the correct answer. We modify only minor attributes such as object type, trajectory, color, count, or location. These changes create subtle perturbations that require precise image understanding. For example:

- **True:** "A black vehicle is going straight."
→ **False:** "A white vehicle is turning right."
- **True:** "Two cars are parked on the right side of the road."
→ **False:** "Five cars are parked on the left side of the road."

3. Each question must have exactly one correct answer.

We manually verify that no false candidate can be interpreted as correct. If a candidate introduces ambiguity or can be considered a valid

Table 8: Ablation Study on Image and Video QA of WaymoQA. Bold: best; underline: second best. The following abbreviations are used: TS (Traffic Signal), SC (Scene Caption), SU (Scene Understanding), PL (Planning), PE (Perception), PR (Prediction), PP (Perception&Prediction), CF (Counterfactual), SE (Special Event), SR (Spatial Relationship), TG (Temporal Grounding), UN (Uncertainty), FT (Fine-tuning).

| Image QA | | | | | | | | | | | | | | | | | | |
|-------------------------------|---------------|--------------|-------------|-------------|-------------|-------------|-------------|-------------|-------------|-------------|-------------------|-------------|-------------|-------------|-------------|-------------|-------------|-------------|
| Model | Train Dataset | Normal Scene | | | | | | Others | | | Safety - Critical | | | | | | Overall | |
| | | TS | SC | SU | PL | PP | Overall | CF | SE | Overall | SU | PE | PR | PL | SC | UN | | Overall |
| Random Guess | - | 25.0 | 25.0 | 25.0 | 25.0 | 25.0 | 25.0 | 25.0 | 25.0 | 25.0 | 25.0 | 25.0 | 25.0 | 25.0 | 25.0 | 25.0 | 25.0 | 25.0 |
| Human Experts | - | 96.6 | 97.7 | 97.7 | 95.3 | 94.0 | 96.1 | 94.8 | 96.7 | 96.3 | 96.8 | 98.0 | 96.4 | 94.3 | 98.7 | 94.9 | 96.0 | 96.1 |
| Qwen2.5-VL(7B) [5] (Baseline) | - | 77.4 | 77.4 | 71.2 | 48.4 | 63.3 | 68.1 | 43.5 | 58.9 | 55.6 | 54.4 | 55.3 | 71.0 | 64.0 | 43.0 | 54.6 | 61.1 | 62.4 |
| Qwen2.5-VL(7B) [5] (FT, Ours) | Image&Video | 84.4 | 72.6 | <u>72.0</u> | 58.5 | 80.6 | 74.9 | 63.1 | 74.8 | 72.7 | 76.1 | 76.6 | 77.8 | 65.9 | 67.8 | 63.8 | 71.2 | 72.9 |
| Qwen2.5-VL(7B) [5] (FT, Ours) | Image | <u>79.1</u> | <u>78.5</u> | 73.6 | <u>53.9</u> | <u>71.1</u> | <u>71.3</u> | <u>49.1</u> | <u>61.5</u> | <u>59.3</u> | <u>61.6</u> | <u>64.0</u> | <u>73.9</u> | <u>64.9</u> | <u>44.3</u> | <u>54.3</u> | <u>63.6</u> | <u>65.7</u> |
| Qwen2.5-VL(7B) [5] (FT, Ours) | Video | 78.6 | 80.0 | 71.6 | 50.4 | 66.7 | 68.7 | 46.4 | 59.1 | 56.8 | 59.4 | 59.3 | 70.9 | 62.0 | 43.7 | <u>54.8</u> | 61.3 | 63.4 |

| Video QA | | | | | | | | | | | | | | | | | | |
|-------------------------------|---------------|--------------|-------------|-------------|-------------|-------------|-------------|-------------|-------------|-------------|-------------------|-------------|-------------|-------------|-------------|-------------|-------------|-------------|
| Model | Train Dataset | Normal Scene | | | | | Others | | | | Safety - Critical | | | | | | Overall | |
| | | TS | SC | SU | PP | Overall | CF | SE | SR | Overall | SC | SU | PE | TG | UN | Overall | | |
| Random Guess | - | 25.0 | 25.0 | 25.0 | 25.0 | 25.0 | 25.0 | 25.0 | 25.0 | 25.0 | 25.0 | 25.0 | 25.0 | 25.0 | 25.0 | 25.0 | 25.0 | 25.0 |
| Human Experts | - | 95.4 | 95.7 | 100.0 | 98.7 | 96.9 | 95.9 | 100.0 | 90.5 | 96.6 | 97.2 | 97.2 | 96.0 | 94.0 | 92.5 | 95.9 | 96.5 | 96.5 |
| Qwen2.5-VL(7B) [5] (Baseline) | - | 80.0 | <u>41.1</u> | <u>70.6</u> | 76.6 | <u>72.7</u> | 48.0 | 89.2 | 52.3 | 64.4 | 32.4 | 53.1 | 55.7 | 31.3 | 64.5 | 49.5 | 63.8 | 63.8 |
| Qwen2.5-VL(7B) [5] (FT, Ours) | Image&Video | 84.0 | 64.7 | 70.7 | 81.6 | 76.0 | 80.0 | 95.8 | 61.9 | 83.1 | 63.5 | 66.2 | 63.5 | 58.9 | <u>70.8</u> | 65.0 | 72.8 | 72.8 |
| Qwen2.5-VL(7B) [5] (FT, Ours) | Image | 78.0 | 35.3 | 68.8 | 76.7 | 71.4 | 48.0 | <u>91.5</u> | 52.4 | 66.1 | 33.8 | <u>58.0</u> | 51.0 | 36.3 | 71.9 | 52.9 | 63.9 | 63.9 |
| Qwen2.5-VL(7B) [5] (FT, Ours) | Video | <u>81.0</u> | <u>41.1</u> | <u>69.1</u> | <u>77.9</u> | 72.6 | <u>51.0</u> | <u>91.5</u> | <u>54.8</u> | <u>67.8</u> | <u>37.9</u> | 56.6 | <u>59.6</u> | <u>39.2</u> | 68.8 | <u>54.1</u> | <u>65.1</u> | <u>65.1</u> |

answer under certain contexts, we revise or discard it.

4. All choices must follow a consistent writing style. Since multiple annotators contribute to the dataset, differences in tone and phrasing naturally occur. A final reviewer rewrites all answer options to unify the style across the dataset. This process ensures that sentence structure, wording, and perspective remain consistent across all choices.

D Ablation Study

Ablation on training modality. Table 8 analyzes how the choice of training modality affects performance on WaymoQA. Starting from the off-the-shelf Qwen2.5-VL(7B) baseline, we fine-tune three variants: (i) on both Image and Video QA data, (ii) on Image QA only, and (iii) on Video QA only.

For **Image QA**, all fine-tuned models outperform the baseline (62.4% overall), but the joint Image&Video model is clearly the most effective. Training only on images raises overall Image QA accuracy to 65.7%, while training only on videos yields 63.4%. In contrast, using both modalities pushes Image QA to 72.9% overall and improves every scene type: normal scenes from 68.1% to 74.9%, “Others” from 55.6% to 72.7%, and safety-critical scenes from 61.1% to 71.2%. Thus, even for image-only evaluation, exposure to video questions provides a substantial gain, especially on safety-critical categories.

A similar trend appears for **Video QA**. Fine-tuning on video-only data improves the baseline from 62.6% to 65.1% overall, and

image-only training gives a smaller boost to 63.9%. However, the Image&Video model again achieves the best result with 72.8% overall accuracy, lifting normal scenes from 72.7% to 76.0%, “Others” from 65.2% to 83.1%, and safety-critical scenes from 51.3% to 65.0%.

These results confirm our hypothesis from the main text: while modality-specific fine-tuning helps the corresponding evaluation modality, jointly training on both image and video questions yields the largest improvements, particularly for safety-critical reasoning, by encouraging the model to share representations across complementary temporal and spatial cues.

E Failure Case.

Figure 6 illustrates a typical failure pattern of our model. In the first stage of Safety-Critical Reasoning, the model correctly identifies the primary safety-critical object (a person and a dog next to the parked vehicle), predicts that the person will remain standing near the car, and concludes that the ego vehicle should wait until the person either walks away or re-enters the vehicle. Thus, basic perception, prediction, and planning around the first hazard are handled reliably.

However, the second stage exposes a systematic weakness when directions are defined in a *relative* coordinate frame. The additional safety-critical object is an oncoming blue vehicle, described in the ground truth as “driving in the opposite lane to the left of the white vehicle in front” and “attempting to drive straight ahead to the left of the white vehicle in front.” Our model instead predicts that the blue vehicle is on the right side of the white vehicle and moving to the right. In other words, it fails to reinterpret “left” and “right”

from the other vehicle’s perspective and mistakenly projects them into the ego-centric frame. This misinterpretation then propagates to downstream sub-questions: the model’s subsequent plan for “addressing the first risk while also addressing the second risk” is inconsistent with the true geometry of the scene, leading to an unsafe recommendation. A similar confusion appears in the normal reasoning question at the bottom of the figure, where the model again flips the turning direction of the rear vehicle when the description is given from that vehicle’s viewpoint.

F Extending WaymoQA

Our current benchmark evaluates *perception*, *prediction*, and *planning* with separate questions. For example, in the scenario shown in Fig. 6, we ask (i) which object is safety-critical, (ii) how that object will move, and (iii) how the ego vehicle should drive safely. While this decomposition reveals which sub-skill fails, it does not explicitly enforce that the model maintains a coherent reasoning chain from perception to planning. A model can sometimes answer each sub-question in isolation by pattern matching, without truly understanding how its perception of agents constrains future motion and, in turn, ego decisions.

Because WaymoQA contains rich, temporally aligned annotations, we can instead reorganize these items into *compound* questions that evaluate the full decision process. For instance, rather than three separate questions, a single multi-part query could ask: (1) which agents are safety-critical in the current scene, (2) how each of them is likely to move over the next few seconds, and (3) which maneuver the ego vehicle should take to reduce overall risk. The ground truth already contains all of this information, so the model’s answer can be graded both holistically and at the level of partial credit: a model that correctly identifies the primary hazard but mispredicts the second agent’s motion would receive credit for perception but be penalized on prediction and planning. Such structured supervision directly ties mistakes in downstream planning to specific upstream errors, e.g., misinterpreting a relative left/right description for an oncoming vehicle.

We view these extensions as a natural next step for WaymoQA. By transforming our existing annotations into multi-stage, chain-structured questions with explicit partial scoring, future work can train and test models on *complete* safety-critical reasoning pipelines rather than isolated sub-tasks, and thus more directly target the types of compounding failures observed in our error analysis.



1st Stage Safety-Critical Reasoning

Question: What is a safety-critical object?

GT: B. A person and a dog standing on the left side of a vehicle parked on the right shoulder ahead.



Ours: B. A person and a dog standing on the left side of a vehicle parked on the right shoulder ahead.

Question: How do you think a safety-critical object will move?

GT: D. It seems like it will stand (bending over and standing while fiddling with something inside the car)



Ours: D. It seems like it will stand (bending over and standing while fiddling with something inside the car)

Question: What should Ego do to drive safely?

GT: B. Ego must wait until this person moves on foot or gets back into the vehicle



Ours: B. Ego must wait until this person moves on foot or gets back into the vehicle..

2nd Stage Safety-Critical Reasoning

Question: Is there any other safety-critical object besides the first safety-critical object? If so, how will it be moved?

GT: B. A blue vehicle is driving in the opposite lane to the left of the front. It is attempting to drive straight ahead to the **left** of the white vehicle in front.



Ours: C. A blue vehicle is driving in the opposite lane to the right of the front. It is attempting to drive straight ahead to the **right** of the white vehicle in front.

Question: How should I drive to address the first risk while also addressing the second risk?

GT: A. Ego must wait until this person moves on foot or gets back into the vehicle.



Ours: D. It is safe to stop, but it is also possible to move to the left.

Normal Reasoning

Question: Based on the current appearance of vehicle, how do they intend to move?

GT: C. The black car in the rear is turning **left** at the intersection.



Ours: A. The black car in the rear is turning **right** at the intersection.

Figure 6: Failure case on two-stage Safety-Critical Reasoning in WaymoQA.